Water Research 220 (2022) 118712

Contents lists available at ScienceDirect

Water Research

journal homepage: www.elsevier.com/locate/watres

Genotype-dependent kinetics of enterovirus inactivation by free chlorine and ultraviolet (UV) irradiation

Shotaro Torii [a,b,*], Marie-Hélène Corre [a], Fuminari Miura [c,d], Masae Itamochi [e], Kei Haga [f], Kazuhiko Katayama [f], Hiroyuki Katayama [b], Tamar Kohn [a]

[a] Laboratory of Environmental Chemistry, School of Architecture, Civil and Environmental Engineering (ENAC), École Polytechnique Fédérale de Lausanne (EPFL), Lausanne, Switzerland
[b] Department of Urban Engineering, School of Engineering, The University of Tokyo, 7-3-1 Hongo, Bunkyo-ku, Tokyo, Japan
[c] Center for Marine Environmental Studies (CMES), Ehime University, Bunkyo-cho 3, Matsuyama-shi, Ehime, Japan
[d] Centre for Infectious Disease Control, National Institute for Public Health and the Environment (RIVM), Bilthoven, the Netherlands
[e] Department of Virology, Toyama Institute of Health, 17-1 Nakataikoyama, Imizu-shi, Toyama, Japan
[f] Laboratory of Viral Infection, Department of Infection Control and Immunology, Ōmura Satoshi Memorial Institute & Graduate School of Infection Control Sciences, Kitasato University, Tokyo 108-8641, Japan

ARTICLE INFO

Keywords:
Virus
Disinfection
Free chlorine
Ultraviolet irradiation
Inactivation
Water treatment

ABSTRACT

Inactivation kinetics of enterovirus by disinfection is often studied using a single laboratory strain of a given genotype. Environmental variants of enterovirus are genetically distinct from the corresponding laboratory strain, yet it is poorly understood how these genetic differences affect inactivation. Here we evaluated the inactivation kinetics of nine coxsackievirus B3 (CVB3), ten coxsackievirus B4 (CVB4), and two echovirus 11 (E11) variants by free chlorine and ultraviolet irradiation (UV). The inactivation kinetics by free chlorine were genotype- (i.e., susceptibility: CVB5 < CVB3 ≈ CVB4 < E11) and genogroup-dependent and exhibited up to 15-fold difference among the tested viruses. In contrast, only minor (up to 1.3-fold) differences were observed in the UV inactivation kinetics. The differences in variability between the two disinfectants could be rationalized by their respective inactivation mechanisms: inactivation by UV mainly depends on the genomic size and composition, which was similar for all viruses tested, whereas free chlorine targets the viral capsid protein, which exhibited critical differences between genogroups and genotypes. Finally, we integrated the observed variability in inactivation rate constants into an expanded Chick-Watson model to estimate the overall inactivation of an enterovirus consortium. The results highlight that the distribution of inactivation rate constants and the abundance of each genotype are essential parameters to accurately predict the overall inactivation of an enterovirus population by free chlorine. We conclude that predictions based on inactivation data of a single variant or reference pathogen alone likely overestimate the true disinfection efficiency of free chlorine.

1. Introduction

Enterovirus is a non-enveloped, positive single-stranded (ss) RNA virus with a diameter of approximately 30 nm. The genus *Enterovirus* consists of more than 100 genotypes infecting humans and causing a broad spectrum of serious illnesses including meningitis, myocarditis, and hand-foot-mouth disease (Bubba et al., 2020). Because they are enteric pathogens, infected individuals shed them into the sewage system and are frequently detected in wastewater and surface waters (Haramoto et al., 2018). Enterovirus is therefore one of the microbial contaminants in Draft Contaminant Candidate List 5 published by the U. S. Environmental Protection Agency (USEPA). Their abundance and reduction/inactivation in water systems has been investigated and analyzed (Boehm et al., 2019; Morrison et al., 2022; Pecson et al., 2022) and often adopted as a reference pathogen in quantitative microbial risk assessment (Lodder et al., 2015; Poma et al., 2019; Schijven et al., 2011).

Water and wastewater treatment are generally expected to reduce infectious virus concentrations to a large extent (e.g., 4-log reduction of viruses for surface water treatment USEPA, 1989). The conventional physical unit processes, such as coagulation-sedimentation, membrane

* Corresponding author at: Laboratory of Environmental Chemistry, School of Architecture, Civil and Environmental Engineering (ENAC), École Polytechnique Fédérale de Lausanne (EPFL), CH-1015 Lausanne, Switzerland.
E-mail address: shotaro.torii@epfl.ch (S. Torii).

https://doi.org/10.1016/j.watres.2022.118712
Received 3 March 2022; Received in revised form 31 May 2022; Accepted 2 June 2022
Available online 4 June 2022

filtration, and sand filtration, have a limited capacity to remove viruses (Asami et al., 2016; Canh et al., 2019; Kato et al., 2018; Yasui et al., 2021). Instead, current treatment trains heavily rely on disinfection (e.g. free chlorine and ultraviolet (UV) irradiation) for virus reduction.

To date, virucidal efficacy of disinfectants were investigated by using laboratory strains (Black et al., 2009; Cromeans et al., 2010; Kahler et al., 2010; Shirasaki et al., 2020; Sobsey et al., 1988; Wati et al., 2018), while environmental variants have only rarely been tested (e.g., Payment et al., 1985; Rodríguez et al., 2022). As a ssRNA virus, *Enterovirus* has a high mutation rate (Sanjuan et al., 2010), suggesting that the amino acid composition of the viral capsid can be diverse even within the same genotype. In light of this, our studies investigated environmental variants of one of the genotypes of *Enterovirus*, coxsackievirus B5 (CVB5), for their inactivation kinetics and observed up to 5-fold variability in free chlorine and up to 1.3-fold variability in UV susceptibility among CVB5 variants (Meister et al., 2018; Torii et al., 2021; Wolf et al., 2018).

To estimate the disinfection efficiency of water and wastewater treatment processes, not only kinetic data for laboratory strains, but also for environmental variants should be considered. We previously proposed an expanded Chick-Watson model that accounts for kinetic variability among variants, to estimate the overall inactivation of a heterogeneous virus consortium. We found that required disinfectant dose to achieve 6-log inactivation of heterogeneous consortium of CVB5 variants was up to 4.2-fold in free chlorine and up to 1.2-fold larger in UV than that of laboratory strain (Torii et al., 2021). However, the model was applied only to a single genotype. Although CVB5 is reported to be one of the most prevalent genotypes in wastewater (Bisseux et al., 2020; Larivé et al., 2021), other genotypes can be dominant depending on the epidemiological situation in the catchment. For example, CVB3 was most frequently isolated in Italian wastewater surveillance (Pennino et al., 2018). Coxsackievirus B4 (CVB4) and Echovirus 11 (E11) were reported as the second and third most prevalent genotypes in wastewater, respectively (Larivé et al., 2021). Therefore, inactivation kinetics of such genotypes are essential to predict the overall inactivation of enterovirus by disinfection processes.

The goal of this work was to evaluate the susceptibility of different variants of CVB3, CVB4, and E11 to common water disinfectants. Specifically, we measured the inactivation kinetics of nine CVB3, ten CVB4, and two E11 variants during inactivation by free chlorine and UV and we identified genetic features that may contribute to altered disinfection susceptibilities. Finally, we modeled the inactivation efficiency of a hypothetical enterovirus consortium as a proof of concept to demonstrate how the disinfection data on environmental isolates can be utilized to estimate the overall inactivation of an enterovirus population.

2. Materials and methods

2.1. Environmental isolates and laboratory strains of enterovirus

A total of nine variants of CVB3 (eight environmental isolates [CVB3.1–CVB3.3, CVB3.5–CVB3.9] and one laboratory strain [CVB3. Nancy]), ten variants of CVB4 (nine environmental isolates [CVB4.1-CVB4.9] and one laboratory strain [CVB4.J.V.B]), two variants of E11 (one environmental isolate [E11.3] and one laboratory strain [E11. Gregory]) were tested in this study. CVB3 Nancy strain and E11 Gregory strain were kindly provided by Prof. Hiroyuki Shimizu (National Institute of Infectious Diseases, Tokyo, Japan). CVB4 J.V.B strain (VR-184™) was purchased from the American Type Culture Collection (ATCC). The environmental isolates were derived from wastewater or a river in Toyama Prefecture, Japan (Iwai et al., 2006; Matsuura et al., 1984), from September 2002 to November 2017. All environmental isolates were sequenced as described previously (Torii et al., 2021). Near full-length genomes were deposited in GenBank database under the accession number MW015027 to MW015034, MW015036 to MW015044, and MW015059. The information (date of isolation and GenBank accession number) on each environmental isolate is presented in Table S1 of the supporting information (SI).

2.2. Virus propagation, purification, and enumeration

Both laboratory strain and environmental isolates were propagated on buffalo green monkey kidney (BGMK) cells to prepare crude virus stocks. Environmental isolates were passaged only once, to obtain a sufficiently high concentration to enable kinetic experiments, while minimizing adaptation to laboratory conditions. The crude stocks were purified by cesium chloride density gradient ultracentrifugation followed by desalting using AmiconUltra 100 kDa (Merck Millipore) as previously described (Torii et al., 2020). This purification method was chosen to minimize virus aggregation (Dika et al., 2013) and chlorine demand (Dunkin et al., 2017) in the viral stock solution. The purified virus stocks were stored at 4 °C until disinfection experiments.

The number of the infective viruses was enumerated by the most probable number (MPN) assay using BGMK cells on 96-well plates (Meister et al., 2018). The samples were serially diluted 10-fold by Eagle's minimum essential medium (Nissui Pharmaceutical, Tokyo, Japan), supplemented with 1% fetal bovine serum (ThermoFisher Scientific, MA, USA). A 150-μL of the diluted sample was inoculated on the BGMK cells, with five replicates per one dilution series. After incubation at 37 °C with 5% CO_2 for six days, the presence of a cytopathic effect in each well was checked by microscopy. The number of positive wells of each dilution series was counted and converted to MPN using R package {MPN} (Ferguson and Ihrie, 2019).

2.3. Genotyping and phylogenetic analysis

Genotyping was performed by RIVM Enterovirus Genotyping Tool Version 1.0, which was classified based on the sequence of the entire VP1 region (Kroneman et al., 2011). Note that the result of the genotype was consistent with that of the serological assay (data not shown). Multiple alignments of the VP1 region (position 2451 to 3380 at CVB3 Nancy strain [M16572], position 2445 to 3299 at CVB4 J.V.B strain [X05690], or position 2459 to 3334 at E11 Gregory strain [X80059]) were constructed by MUSCLE (Edgar, 2004) using the default gap parameters. Bootstrapped, neighbor-joining (Kimura two-parameter model) phylogenetic trees were constructed with pairwise deletion and with 1000 replicates using MEGA X version 10.1.6 (Kumar et al., 2018).

2.4. Modeling of viral capsid protein

The structural accessibility of CVB4 capsid residues was assessed using PDB structure 6CZK (CVB4 Strain E2) (Flatt et al., 2021). The visualization of the capsid, as well as the identification of accessible amino acids, was performed under ChimeraX version 1.3.

2.5. Disinfection experiments

Disinfection experiments were run in duplicate or triplicate for each pair of viruses and disinfectants. A total of four time-series samples, including the sample at time zero, were taken in each run. All experiments were conducted in disinfectant demand-free (DDF) water at 22 ± 1 °C. DDF water was buffered to 10 mM and brought to pH 7.0 by adding Na_2HPO_4 and KH_2PO_4 (FUJIFILM Wako, Tokyo, Japan) into MilliQ water.

2.5.1. Free chlorine

The free chlorine disinfection experiment was conducted in a batch system. A free chlorine working solution was prepared by diluting sodium hypochlorite (FUJIFILM Wako) in DDF water. At pH 7.0, the dominant species of free chlorine is hypochlorous acid (77%). The final free chlorine concentration in the working solution ranged from 0.27 to

0.35 mg L^{-1}. The free chlorine concentration was measured by *N, N*-diethyl-*p*-phenylenediamine (DPD) method using a colorimetric methodology with a DR890 colorimeter (Hach Company, Loveland, CO). Prior to each run, glass beakers were soaked with 50 mg L^{-1} of sodium hypochlorite overnight to quench residual chlorine demand. The beakers were rinsed twice with the working solution. Then, 30 μL of virus stock solution was spiked into a 20 mL working solution under constant stirring, resulting in an initial virus concentration ranging from 10^3 to 5×10^4 MPN mL^{-1}. A 1 mL aliquot was collected every 8 − 45 s (depending on variants) and mixed with 10 μL of 5000 mg L^{-1} of sodium thiosulfate (FUJIFILM Wako) to quench the residual free chlorine. The initial virus concentration was sampled from 20 mL of buffered DDF water without free chlorine, spiked with the same amount (i.e., 30 μL) of virus stock. The 1 ml aliquots were stored at 4 °C until virus enumeration.

The free chlorine concentration was measured at the beginning and the end of each run. The decay in free chlorine concentration was less than 21% throughout each run. The chlorine dose for each sample, expressed as the CT value, was determined by integration of the time-dependent disinfectant concentration over exposure time, assuming the first-order decay in free chlorine concentration between time 0 s and the end of the run.

2.5.2. UV

UV irradiation was performed in batch in a collimated beam low-pressure UV (LPUV) system. The UV system comprised a 15-W LPUV lamp (GL15, Toshiba, Japan) emitting a peak wavelength of 254 nm, a shutter, and an auto-time controller. A 10 mL aliquot of DDF water spiked with 30 μL of virus stock was irradiated in a 5.5 cm diameter Petri dish (1.3 cm depth) with quiescent stirring. The increase in UV_{254} absorbance after spiking purified virus stocks to the DDF water was less than 0.002 cm^{-1}. A 300 μL aliquot was harvested at 0 s, 15 s, 30 s, and 45 s. The harvested samples were stored at 4 °C until virus enumeration. The fluence rate (μW cm^{-2}) was given by multiplying the readings of a radiometer (UVR2 UD25, TOPCON) by the water factor (0.99) and reflection factor (0.975) (Bolton and Linden, 2003) and ranged from 423 to 540 μW cm^{-2}. The UV dose (mJ cm^{-2}) for each sample was determined as a product of the fluence rate and the corresponding exposure time.

2.6. Estimation of inactivation rate constants for each variant

Inactivation rate constants (k) of each variant were estimated by fitting the models shown in Eqs. (1) and (2) in Table 1 to the data of the disinfection experiments. Eqs. (1) and (2) are the Chick–Watson model, where pseudo-first-order kinetics of virus inactivation was assumed with respect to disinfectant dose. The k value of each variant was determined based on the pooled data from all replicates as the slope of $\ln(N/N_0)$ versus disinfectant dose by linear least-squares regression.

2.7. Overall inactivation of each genotype of enterovirus

Overall inactivation of CVB3 and CVB4 were modeled by an expanded Chick-Watson model as described previously (Torii et al., 2021). First, the distribution of k values of the variants of each genotype was determined. To this end, the parameters and Akaike information criterion (AIC) of gamma and lognormal distribution of k were estimated by maximum likelihood estimation using the R package{fitdistrplus} (Delignette-Muller and Dutang, 2015). If the gamma distribution was selected based on AIC, the overall inactivation of the given genotype was modeled as Eq. (3), hereafter named Gamma model.

$$\frac{N}{N_0} = \left(1 + \frac{1}{\beta} D\right)^{-\alpha} \tag{3}$$

where α is the shape parameter, β is the rate parameter, D is the disinfectant dose (i.e., either CT value or UV dose).

If the lognormal distribution was selected, the overall inactivation of the given genotype was modeled as Eq. (4), hereafter named Lognormal model.

$$\frac{N}{N_0} = \frac{1}{\sqrt{1 + \mathscr{W}(e^{\mu}\sigma^2 D)}} \exp\left(- \frac{\{\mathscr{W}(e^{\mu}\sigma^2 D)\}^2 + 2\,\mathscr{W}(e^{\mu}\sigma^2 D)}{2\sigma^2} \right) \tag{4}$$

where μ is the mean, and σ is the standard deviation of the lognormal distribution and $\mathscr{W}(\cdot)$ is the *Lambert W function,* which is defined as the solution of the $\mathscr{W}(x)e^{\mathscr{W}(x)} = x$. The Lambert function was calculated in R using {lamW} (Adler, 2015).

Overall inactivation of the hypothetical enterovirus consortium was given by the arithmetic mean of the inactivation efficiency weighted by the abundance of each genotype.

2.8. Statistical analyses

All statistical analyses were implemented in R-3.6.0.(R Core Team, 2019). Linear least-squares regression was performed with {lm} function to estimate inactivation rate constants from the disinfection experiments. Tukey's honestly significant difference (HSD) test was used to perform the inter-genotype comparison of the log-transformed k. Welch two-sample t-test was performed to compare the log-transformed k between the two genogroups of CVB4. F-test was performed to test the homogeneity of variance between log-transformed k_{FC} and k_{UV}. Comparisons with a P-value < 0.05 were considered significantly different.

Table 1
Inactivation models adopted in this study.

Disinfectant	Inactivation model	Order of reaction
Free chlorine	$\frac{N}{N_0} = e^{-k_{FC}CT}$ (1)	Pseudo-first order
UV	$\frac{N}{N_0} = e^{-k_{UV}ET}$ (2)	Pseudo-first order

N is the infective virus concentration at time T (MPN mL^{-1}), N_0 is the infective virus concentration at time 0 (MPN mL^{-1}), k_{FC} is the inactivation rate constant by free chlorine (mg^{-1} min^{-1} L), k_{UV} is the inactivation rate constant by UV (mJ^{-1} cm^2), C is the free chlorine concentration (mg L^{-1}), E is the fluence rate of UV (mW cm^{-2}), T is the exposure time in the batch reactor (s or min).

3. Results

3.1. Phylogenetic analyses

To genetically overview all the tested variants of CVB3, CVB4, and E11, a phylogenetic tree was constructed as shown in Fig. 1. The nucleotide identities within CVB3, CVB4, and E11 variants in VP1 region ranged from 71.6% to 99.5%, from 75.9% to 98.9%, and 70.3%, respectively (see Table S2). The environmental CVB3, CVB4, and E11 variants shared only <76.7%, <83.4%, and 70.3% of nucleotide identities with the corresponding laboratory strain, all of which were isolated in the 1950s (Table S1). These results highlight that the laboratory strains are not genetically representative of currently circulating environmental enterovirus.

For further analysis, CVB4 variants were divided into two groups, genogroup A, including CVB4.4, CVB4.5, CVB4.1, and CVB4.J.V.B., and genogroup B, CVB4.6, CVB4.8, CVB4.9, CVB4.7, CVB4.2, and CVB4.3. This classification is similar to a previous phylogenetical study of CVB4 (Tian et al., 2014). Genogroup A, defined in this study, is corresponding to genotypes I and V, while genogroup B includes genotypes II, III, IV (Tian et al., 2014).

3.2. Kinetics of inactivation by free chlorine and UV

Fig. 2 (top panels) shows the inactivation rate constants estimated

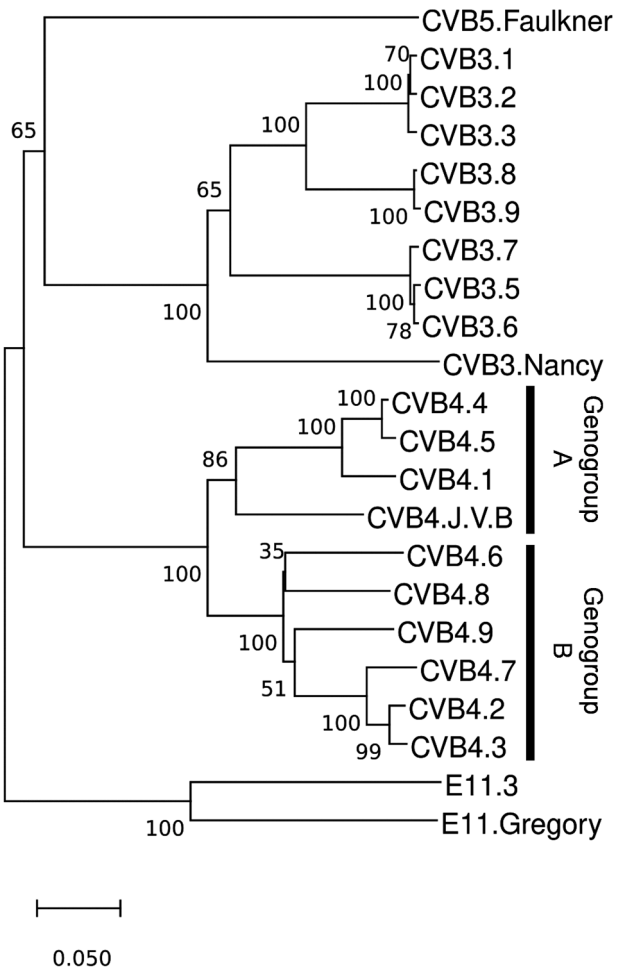

Fig. 1. The phylogenetic tree constructed for the entire VP1 region of CVB3, CVB4, and E11 variants. CVB5 Faulkner strain (Accession number: AF114383) was added for comparison. The percentages of the replicate trees where the associated taxa clustered together in the bootstrap test (1000 replicates) are shown next to the branches.

for each variant from experimental inactivation data (shown in Figs. S1 and S2). Also shown are the inactivation rate constants previously measured for CVB5 variants under the same experimental conditions (Torii et al., 2021). The lower panels of Fig. 2 show the free chlorine CT values or UV dose required for 4-log inactivation of each variant. These CT values or UV doses were extrapolated using the Chick–Watson model, namely, given by $4/k\log_{10}e$. Table S3 shows the data on inactivation rate constants and required CT value or dose for 4-log inactivation of each variant. All inactivation data were provided in a supporting spreadsheet.

The inactivation rate constants by free chlorine (k_{FC}) ranged from 8.55 to 15.4, from 6.87 to 19.8, and from 32.6 to 57.7 mg^{-1} min^{-1} L, for CVB3, CVB4, and E11, respectively. Correspondingly, the predicted CT values for 4-log inactivation ranged from 0.60 to 1.08, from 0.46 to 1.34, and from 0.16 to 0.28 mg min L^{-1}, for CVB3, CVB4, and E11, respectively. Significant differences in free chlorine susceptibility were observed among genotypes with the following order: CVB5 < CVB3 ≈ CVB4 < E11. Interestingly, a significant difference in free chlorine susceptibility was also observed between the two genogroups of CVB4; genogroup B exhibited lower susceptibility than genogroup A, to which CVB4 J.V.B strain belonged ($p < 0.05$) (see Table S3). These results suggest that the free chlorine susceptibility of enterovirus depends on the genogroup or genotype classified based on the similarity of the genomic sequence coding capsid proteins.

The inactivation rate constants (k_{UV}) ranged from 0.31 to 0.39, from 0.29 to 0.39, from 0.307 to 0.311 mJ^{-1} cm^2 in CVB3, CVB4, and E11, respectively. Correspondingly, the predicted UV dose for 4-log inactivation ranged from 24 to 30, from 24 to 32, and from 29.6 to 30.0 mJ cm^{-2}. No significant differences were observed among the variants or genogroups. The predicted UV dose for 4-log inactivation of CVB3 Nancy (i.e., 27.6 mJ cm^{-2}) nd E11 Gregory strain (i.e., 30 mJ cm^{-2}) was comparable with previous reports (i.e., 32.5 and 26.6 mJ cm^{-2} for CVB3 Nancy and E11 Gregory, respectively.) (Gerba et al., 2002; Meister et al., 2018). The predicted UV doses for 4-log inactivation of CVB4 environmental isolates were also comparable with two variants tested in previous work (i.e., 24.5 and 26.1 mJ cm^{-2}) (Meister et al., 2018). No significant inter-genotype difference in UV susceptibility was observed among genotypes: CVB3 ≈ CVB4 ≈ CVB5 ≈ E11.

In summary, the variance of k_{FC} was significantly larger than that of k_{UV} in all the genotypes. Free chlorine susceptibilities differed by up to 15-fold within investigated enterovirus and were variable even within the same genotype. In contrast, UV susceptibility remained within a factor of 1.3 for all viruses tested. No significant difference in UV susceptibility was observed even among genotypes.

4. Discussion

4.1. Underlying causes of genotype-, genogroup-dependent kinetics of inactivation by free chlorine and UV

For enterovirus to be infective, it should be capable of (i) binding to receptors expressed on the host cells, (ii) uncoating virions and releasing viral genomic RNA into the cytoplasm, and (iii) replicating in the host cells. All these functionalities must be intact to fulfill a viral life-cycle (Wigginton et al., 2012). In light of this, the genotype-, genogroup-dependent difference in inactivation kinetics can be attributable to the difference in the integrity of one (or several) of the functionalities.

4.1.1. Free chlorine

Several studies have attempted to unravel the inactivation mechanism of enterovirus by free chlorine (Alvarez and O'Brien, 1982; Nuanualsuwan and Cliver, 2003). Most of them revealed the main contribution of capsid damage to the inactivation. Torrey et al. observed that loss of viral RNA functionality (i.e., replication in the host cell, defined as (iii) in the above paragraph) contributed 38% to the overall inactivation rate of E11 Gregory strain (Torrey et al., 2019), indicating that the remaining can be explained by the other two functionality losses. Another functionality test of E11 Gregory strain showed that loss of binding capacity contributed 70% to the overall inactivation rate (Zhong et al., 2017). A difference in free chlorine susceptibility among variants may thus be attributable to the difference in the integrity of the binding and uncoating functionalities.

Group B Coxsackievirus generally infects host cells by attaching to coxsackievirus-adenovirus receptor (CAR) and inducing conformational changes in the viral capsid and mediating uncoating (Bergelson et al., 1997). Structural analyses showed that the CAR binds at the surface depression ("canyon") present in each icosahedral 5-fold vortex (Muckelbauer et al., 1995a; Verdaguer et al., 2003). For example, the binding of CAR to CVB1 is mediated by five hydrogen bonds and several van der Waals contacts between CAR and the VP1 BCE/EF/GH loops, VP2 EF loop, and VP3 GH loop from two adjacent protomers (Xu et al., 2021).

Inter-genogroup differences in free chlorine susceptibility observed in CVB4 can be explained by the amino acid substitutions around these attachment sites. Common amino acid substitutions between genogroup A and B of CVB4 are shown in Table 2. S154Q at VP2 and M93K/T at VP3 are substitutions of chlorine-reactive by stable amino acids (Pattison and Davies, 2001). A capsid model of CVB4 reveals that these two residues are surface-exposed and accessible to disinfectant (Figure S3).

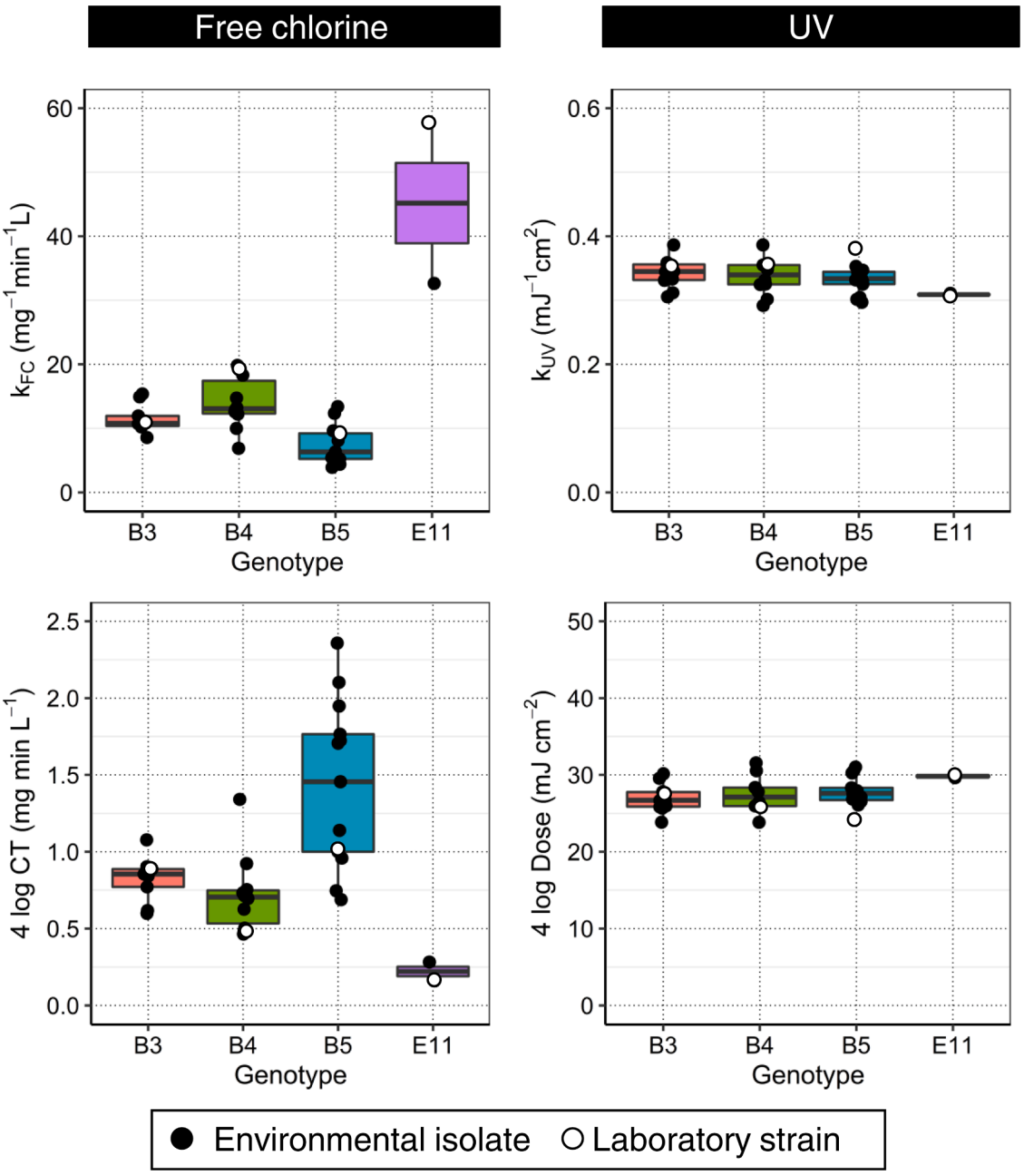

Fig. 2. (Top panels) The inactivation rate constants estimated for each variant from experimental inactivation data. (Lower panels) Predicted free chlorine CT values and UV doses for 4-log inactivation of each variant. The experiments were performed at pH 7.0 at 22 ± 1 °C. The data on CVB5 variants are cited from our previous study (Table S3 in Torii et al., 2021) performed under the same experimental conditions as the present study.

Table 2
Common amino acid substitutions between genogroup A and B of CVB4. Location was assumed from the crystal structure of CVB3 M strain (Muckelbauer et al., 1995a).

Protein	Residue	Amino acid		Location
		Genogroup A	Genogroup B	
VP2	154	S	Q	EF loop (puff)
VP3	93	M	K/T	Knob
VP1	5	E	D	N terminus[a]

[a] This residue is located on the inner surface of the viral capsid and is assumingly disordered (Muckelbauer et al., 1995b).

S154Q at VP2 is located on the EF loop, which is putatively related to CAR binding (Xu et al., 2021). M93K/T at VP3 is located on the knob, which is putatively related to other cell binding sites (i.e., decay-accelerating factor) (Gullberg et al., 2010). Interestingly, our previous data indicate that more chlorine-susceptible CVB5 variants have substitutions from M to L/S/T at the same position of the VP3 knob (Torii et al., 2021). We speculate that these substitutions reduce the chlorine reactivity of attachment sites, leading to a slower decay of the binding functionality of viruses of CVB4 genogroup B compared to genogroup A, and hence to an enhanced chlorine tolerance.

Further studies are needed to confirm the effect of specific amino acid substitutions and receptor usage on free chlorine susceptibility. A mechanism of genotype-dependent susceptibilities may be also explained by the amino acid substitutions around attachment and uncoating site, although a specific site could not be identified due to a

large number of common amino acid substitutions among genotypes.

4.1.2. UV

Inactivation of enterovirus by UV has been reported to occur mainly by the damage of viral RNA, inhibiting replication in the host cells (Rockey et al., 2020; Young et al., 2019). Previous studies reported that UV induces photochemical reactions at pyrimidine bases (Qiao and Wigginton, 2016). Recently, a total number of reactive bases (e.g., number of cytosines (C), uracil (U), uracil doublets (UU), and uracil triplets (UUU) (Rockey et al., 2021)) was reported as an indicator for UV susceptibility of single-stranded RNA viruses (Cheng et al., 2021; Qiao et al., 2018; Rockey et al., 2021; Ye et al., 2018). In light of this, all the tested CVB3 and CVB4 variants were examined for total reactive bases (i.e., the number of U, C, UU, and UUU) (see Table S4). The ratio of reactive to total bases was comparable among all viruses tested, ranging from 0.55 to 0.56. These comparable UV reactivities of the genome can explain the enteroviruses' similar susceptibilities to UV.

4.2. Prediction of overall inactivation efficiency and changes in population composition

Most estimates of overall inactivation efficiency have been based on a single or a few data of a certain variant in the reference pathogen. For example, chlorination efficiency of overall norovirus inactivation was estimated by literature data on the susceptibility of a single variant of Calicivirus, Murine Norovirus 1 (Sokolova et al., 2015). The result of the present study highlights the importance of investigating the inactivation kinetics of different variants and genotypes of a given reference pathogen.

Measurement of the inactivation kinetics of environmental variants allows for predicting the overall disinfection efficiency of enterovirus populations and for assessing the change in population composition

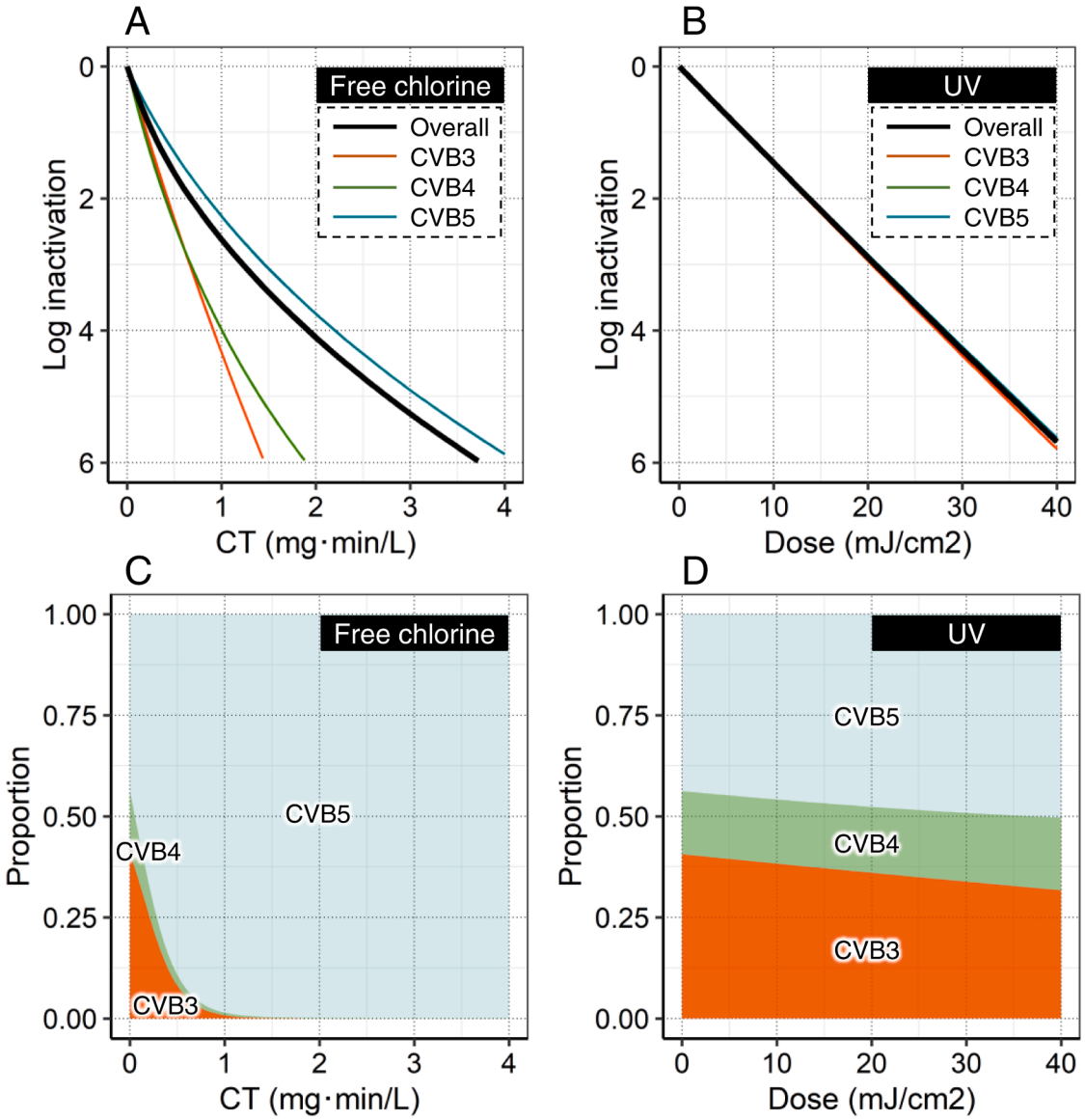

Fig. 3. Computed inactivation curves of an enterovirus consortium (CVB3, CVB4, and CVB5) and population composition as a function of disinfectant dose. (A, B) Inactivation curves for the overall population and each enterovirus genotype by free chlorine (pH 7.0 at 22 °C) (A) and by UV (B). The bold black line indicates the overall inactivation of the enterovirus consortium. Orange-, green-, and blue lines represent CVB3, CVB4, and CVB5 inactivation, respectively. Inactivation of CVB5 was cited from our previous report (Torii et al., 2021). (C, D) Change in genotype composition in the enterovirus consortia as a function of CT value (C) of free chlorine (pH 7.0 at 22 °C) and dose of UV (D). Orange-, green-, blue-shaded areas indicate the proportion of CVB3, CVB4, CVB5. The initial proportion corresponded to CVB3: CVB4: CVB5 = 0.406: 0.156: 0.438).

during disinfection. To further demonstrate this, we simulated the inactivation and composition of a hypothetical enterovirus consortium (consisting of variants of CVB3, CVB4, and CVB5) as a function of disinfectant dose (Fig. 3). Herein, the hypothetical enterovirus consortium was assumed according to previous wastewater surveillance reporting that CVB3, CVB4, and CVB5 were detected at the ratio of 0.406:0.156:0.438 in wastewater influent (Battistone et al., 2014). Note that E11 was removed from this analysis because of limited data on variant disinfection kinetics for parameter estimation.

Based on the AIC comparisons (see Table S5), Gamma models were selected for representing the inactivation of CVB4 by free chlorine and that of all the genotypes by UV, while Lognormal models were applied for depicting inactivation of CVB3 and CVB5 by free chlorine.

Fig. 3A, B shows the computed inactivation curves of CVB3, CVB4, and CVB5 by free chlorine and UV, respectively. The corresponding model parameters are presented in Table S6. Free chlorine inactivation of CVB3 and CVB4 was faster than that of CVB5. The predicted CT values for 4-log inactivation of CVB3, CVB4, and CVB5 were 0.91, 1.01, and 2.20 mg min L^{-1}, respectively. The CT values for 4-log overall inactivation of the enterovirus consortium were predicted as 1.92 mg min L^{-1}, which is smaller than USEPA guidance manual CT values to achieve 4-log inactivation at 22 °C at pH 6–9 (i.e., 2.6 mg min L^{-1}) (USEPA, 2002). The guidance values to achieve 4-log inactivation thus remain protective, though the protectiveness can be lowered if the chlorination is performed at higher pH than pH 7 and/or to achieve higher inactivation than 4-log. An interesting point of this modeling is the difference in the shape of inactivation curve between CVB3 and CVB4. Based on the disinfection experiments, the mean k_{FC} of CVB4 is slightly larger than that of CVB3. Correspondingly, at lower CT (i.e., $<$ 0.61 mg min L^{-1}), CVB4 is predicted to inactivate with higher efficiency than CVB3. However, the trend changes at CT of 0.61 mg min L^{-1}, and the inactivation efficiency of CVB4 diminishes below that of CVB3. This is because of the larger variance of k_{FC} of CVB4. Higher variability causes a more pronounced tailing of inactivation curve. For the prediction of virus reduction through water treatment, a mean or minimum reduction value of a given pathogen is typically of central importance (Schmidt et al., 2020). The difference in CVB3 and CVB4 inactivation alarms such a trend and highlights the importance of investigating the variance of k within a given reference pathogen.

UV inactivations of CVB3, CVB4, and CVB5 were comparable. The doses for 4-log inactivation of CVB3, CVB4, and CVB5 were 27, 28, and 28 mJ cm^{-2}, respectively. Accordingly, the predicted dose for 4-log overall inactivation of the enterovirus consortium was similar (28 mJ cm^{-2}).

The data on the inactivation kinetics of each genotype is also useful to assess the change in the abundance of different genotypes. Fig. 3C, D indicates the change in population composition during the disinfection. Compared with the initial population (i.e., CVB3: CVB4: CVB5 = 0.406: 0.156: 0.438), the proportion of CVB3 and CVB4 decreased and that of CVB5 became dominant as the free chlorine dose increased. For example, at 4-log overall inactivation, CVB3: CVB4: CVB5 is estimated to be present at a ratio of 1.1×10^{-4}: 1.5×10^{-3}: 0.998. On the other hand, the composition of CVB3, CVB4, and CVB5 stayed relatively stable during UV disinfection due to their comparable inactivation kinetics.

It should be noted that there is some room for improvement in the simulation. For example, the simulation could integrate more data on the abundance of each genotype and the inactivation kinetics. Recent advancements in next-generation sequencing could add information on the abundance of more genotypes of enterovirus in wastewater (Bisseux et al., 2020; Brinkman et al., 2017). The inactivation kinetics of different genotypes can be further tested by using environmental isolates as was done in this study. Moreover, the model should be generalized to be applicable under other physicochemical conditions than those used herein. For instance, a previous study reported that the inactivation by free chlorine proceeds slower as the pH increases from 6 to 8, due to the shift in speciation between hypochlorous acid, which has a high virucidal efficiency, and the less efficient hypochlorite ion (Sobsey et al., 1988). Inactivation may proceed more slowly than expected due to shielding exerted by the matrix (e.g., turbidity Templeton et al., 2005; Wati et al., 2018), in particular in wastewater. Incorporation of these effects into the model allows for a more accurate prediction of the enterovirus inactivation.

4.3. Implications for the prediction of virus inactivation by disinfection

This study assessed the variability in inactivation kinetics of enterovirus variants by free chlorine and UV and observed different variability between the two disinfectants. The finding provides implications for a more accurate prediction of virus inactivation during disinfection processes.

Prediction of the enterovirus inactivation by UV is relatively robust to biological variability. Recent studies showed that the inactivation kinetics of ssRNA virus was predictable with high accuracy by a multiple linear regression model taking the number of several pyrimidine-based sequence combinations as predictors (Cheng et al., 2021; Rockey et al., 2021). Moreover, several studies reported similar inactivation kinetics among variants of several enterovirus genotypes (Gerba et al., 2002; Meister et al., 2018). Given that enterovirus generally has a similar genomic length with similar GC contents, the UV susceptibility seems to be comparable among variants of enterovirus. The prediction of enterovirus inactivation by UV is likely to be robust to the change in the population of enterovirus in the source water.

Contrary to UV, free chlorine susceptibility differed among genotypes, genogroups, and even variants. This casts doubt on the suitability of the current prediction scheme; inactivation of a certain viral pathogen is predicted based on the inactivation data of a single or a limited number of variants. Free chlorine is one of the most common disinfectants for water and wastewater treatment, yet its efficiency against the viruses that have not been tested is difficult to predict (Qiao et al., 2022). Further studies need to confirm the relationship between capsid oxidation and functional loss of CVB5 from structural and functional viewpoints (Wigginton and Kohn, 2012). This finding deepens the understanding of the inactivation mechanism by free chlorine and the relationship between capsid composition, structure, and disinfection susceptibilities.

Further research should address biological variability in disinfection and explain the genotype-dependent difference in inactivation kinetics by free chlorine. Concurrence of amino acid substitutions among genotypes observed in this study made it difficult to specify key amino acids associated with chlorine tolerance. A detailed investigation of this field supports the rationale of using the expanded Chick-Watson model to predict the overall inactivation of a given type of virus.

5. Conclusions

The disinfection susceptibilities among enterovirus were genotype- (i.e., susceptibility: CVB5 $<$ CVB3 $\approx$ CVB4 $<$ E11), genogroup- and variant-dependent in free chlorine (i.e., up to 15-fold difference within tested variants) while they were relatively comparable in UV (i.e., up to 1.3-fold difference within tested variants). The differences in variability among disinfectants were assumingly due to those in the inactivation mechanism; kinetics of enterovirus inactivation by UV mainly depends on the genomic composition, whereas that by free chlorine depends on the capsid structure. A large dataset of the genotype abundance and the inactivation kinetics of each enterovirus genotype (i.e., distribution of k value) allows for predicting the overall inactivation more accurately.

Associated information

Supporting figures and tables were supplied as Supporting Information. All inactivation data were provided in a supporting spreadsheet.

Declaration of Competing Interest

The authors declare that they have no known competing financial interests or personal relationships that could have appeared to influence the work reported in this paper.

Acknowledgment

This work was supported by the funding from Japan Society for the Promotion of Science (JSPS KAKENHI, Grant 20H00259, 20J10268, 20J00793), JSPS Overseas Challenge Program for Young Researchers, Young Researchers Exchange Programme between Japan and Switzerland (EGJP_04–042020), and JSPS Overseas Research Fellowships. We appreciate Dr. Hiroyuki Shimizu (National Institute of Infectious Diseases, Tokyo, Japan) for providing us with coxsackievirus B3 Nancy strain and E11 Gregory strain.

Supplementary materials

Supplementary material associated with this article can be found, in the online version, at doi:10.1016/j.watres.2022.118712.

References

Adler, A., 2015. LamW. Lambert-W Function.
Alvarez, M.E., O'Brien, R.T., 1982. Effects of chlorine concentration on the structure of poliovirus. Appl. Environ. Microbiol. 43, 237–239.
Asami, T., Katayama, H., Torrey, J.R., Visvanathan, C., Furumai, H., 2016. Evaluation of virus removal efficiency of coagulation-sedimentation and rapid sand filtration processes in a drinking water treatment plant in Bangkok, Thailand. Water Res. 101, 84–94. https://doi.org/10.1016/j.watres.2016.05.012.
Battistone, A., Buttinelli, G., Bonomo, P., Fiore, S., Amato, C., Mercurio, P., Cicala, A., Simeoni, J., Foppa, A., Triassi, M., Pennino, F., Fiore, L., 2014. Detection of enteroviruses in influent and effluent flow samples from wastewater treatment plants in Italy. Food Environ. Virol. 6, 13–22. https://doi.org/10.1007/s12560-013-9132-2.
Bergelson, J.M., Cunningham, J.A., Droguett, G., Kurt-Jones, E.A., Krithivas, A., Hong, J. S., Horwitz, M.S., Crowell, R.L., Finberg, R.W., 1997. Isolation of a common receptor for coxsackie B viruses and adenoviruses 2 and 5. Science 275, 1320. https://doi.org/10.1126/science.275.5304.1320, 80-.LP –1323.
Bisseux, M., Didier, D., Audrey, M., Christine, A., Hélène, P.L., Jean-Luc, B., Cécile, H., 2020. Monitoring of enterovirus diversity in wastewater by ultra-deep sequencing: an effective complementary tool for clinical enterovirus surveillance. Water Res. 169, 115246 https://doi.org/10.1016/j.watres.2019.115246.
Black, S., Thurston, J.A., Gerba, C.P., 2009. Determination of Ct values for chlorine of resistant enteroviruses. J. Environ. Sci. Heal. Part A Toxic Hazard. Subst. Environ. Eng. 44, 336–339. https://doi.org/10.1080/10934520802659653.
Boehm, A.B., Silverman, A.I., Schriewer, A., Goodwin, K., 2019. Systematic review and meta-analysis of decay rates of waterborne mammalian viruses and coliphages in surface waters. Water Res. 164, 114898 https://doi.org/10.1016/j.watres.2019.114898.
Bolton, J.R., Linden, K.G., 2003. Standardization of methods for fluence (UV Dose) determination in bench-scale UV experiments. J. Environ. Eng. 129, 209–215. https://doi.org/10.1061/(ASCE)0733-9372(2003)129:3(209).
Brinkman, N.E., Fout, G.S., Keely, S.P., 2017. Retrospective surveillance of wastewater to examine seasonal dynamics of enterovirus infections. mSphere 2, e00099. https://doi.org/10.1128/mSphere.00099-17, 17.
Bubba, L., Broberg, E.K., Jasir, A., Simmonds, P., Harvala, H., Redlberger-Fritz, M., Nikolaeva-Glomb, L., Havlíčková, M., Rainetova, P., Fischer, T.K., Midgley, S.E., Epštein, J., Blomqvist, S., Böttcher, S., Keeren, K., Bujaki, E., Farkas, Á., Baldvinsdóttir, G.E., Morley, U., De Gascun, C., Pellegrinelli, L., Piralla, A., Martinuka, O., Zamjatina, N., Griškevičius, A., Nguyen, T., Dudman, S.G., Numanovic, S., Wieczorek, M., Guiomar, R., Costa, I., Cristina, T., Bopegamage, S., Pastuchova, K., Berginc, N., Cabrerizo, M., González-Sanz, R., Zakikhany, K., Hauzenberger, E., Benschop, K., Duizer, E., Dunning, J., Celma, C., McKenna, J., Feeney, S., Templeton, K., Moore, C., Cottrell, S., 2020. Circulation of non-polio enteroviruses in 24 EU and EEA countries between 2015 and 2017: a retrospective surveillance study. Lancet Infect. Dis. 20, 350–361. https://doi.org/10.1016/S1473-3099(19)30566-3.
Canh, V.D., Furumai, H., Katayama, H., 2019. Removal of pepper mild mottle virus by full-scale microfiltration and slow sand filtration plants. NPJ Clean Water 2, 18. https://doi.org/10.1038/s41545-019-0042-1.
Cheng, S., Ge, Y., Lee, Y., Yang, X., 2021. Prediction of photolysis kinetics of viral genomes under UV254 irradiation to estimate virus infectivity loss. Water Res. 198, 117165 https://doi.org/10.1016/j.watres.2021.117165.
Cromeans, T.L., Kahler, A.M., Hill, V.R., 2010. Inactivation of adenoviruses, enteroviruses, and murine norovirus in water by free chlorine and monochloramine. Appl. Environ. Microbiol. 76, 1028–1033. https://doi.org/10.1128/AEM.01342-09.
Delignette-Muller, M.L., Dutang, C., 2015. fitdistrplus: an R package for fitting distributions. J. Stat. Softw. 64, 1–34.
Dika, C., Gantzer, C., Perrin, a, Duval, J.F., 2013. Impact of the virus purification protocol on aggregation and electrokinetics of MS2 phages and corresponding virus-like particles. Phys. Chem. Chem. Phys. 15, 5691–5700. https://doi.org/10.1039/c3cp44128h.
Dunkin, N., Weng, S., Jacangelo, J.G., Schwab, K.J., 2017. Minimizing bias in virally seeded water treatment studies: evaluation of optimal bacteriophage and mammalian virus preparation methodologies. Food Environ. Virol. 9, 473–486. https://doi.org/10.1007/s12560-017-9307-3.
Edgar, R.C., 2004. MUSCLE: multiple sequence alignment with high accuracy and high throughput. Nucl. Acids Res. 32, 1792–1797. https://doi.org/10.1093/nar/gkh340.
Ferguson, M., Ihrie, J., 2019. MPN: most probable number and other microbial enumeration techniques.
Flatt, J.W., Domanska, A., Seppälä, A.L., Butcher, S.J., 2021. Identification of a conserved virion-stabilizing network inside the interprotomer pocket of enteroviruses. Commun. Biol. 4, 250. https://doi.org/10.1038/s42003-021-01779-x.
Gerba, C.P., Gramos, D.M., Nwachuku, N., 2002. Comparative inactivation of enteroviruses and adenovirus 2 by UV light. Appl. Environ. Microbiol. 68, 5167. https://doi.org/10.1128/AEM.68.10.5167-5169.2002. LP –5169.
Gullberg, M., Tolf, C., Jonsson, N., Mulders, M.N., Savolainen-Kopra, C., Hovi, T., Van Ranst, M., Lemey, P., Hafenstein, S., Lindberg, A.M., 2010. Characterization of a putative ancestor of coxsackievirus B5. J. Virol. 84, 9695. https://doi.org/10.1128/JVI.00071-10. LP –9708.
Haramoto, E., Kitajima, M., Hata, A., Torrey, J.R., Masago, Y., Sano, D., Katayama, H., 2018. A review on recent progress in the detection methods and prevalence of human enteric viruses in water. Water Res. 135, 168–186. https://doi.org/10.1016/j.watres.2018.02.004.
Iwai, M., Yoshida, H., Matsuura, K., Fujimoto, T., Shimizu, H., Takizawa, T., Nagai, Y., 2006. Molecular epidemiology of echoviruses 11 and 13, based on an environmental surveillance conducted in toyama prefecture, 2002-2003. Appl. Environ. Microbiol. 72, 6381. https://doi.org/10.1128/AEM.02621-05. LP –6387.
Kahler, A.M., Cromeans, T.L., Roberts, J.M., Hill, V.R., 2010. Effects of source water quality on chlorine inactivation of adenovirus, coxsackievirus, echovirus, and murine norovirus. Appl. Environ. Microbiol. 76, 5159–5164. https://doi.org/10.1128/AEM.00869-10.
Kato, R., Asami, T., Utagawa, E., Furumai, H., Katayama, H., 2018. Pepper mild mottle virus as a process indicator at drinking water treatment plants employing coagulation-sedimentation, rapid sand filtration, ozonation, and biological activated carbon treatments in Japan. Water Res. 132, 61–70. https://doi.org/10.1016/j.watres.2017.12.068.
Kroneman, A., Vennema, H., Deforche, K., Avoort, H.v.d., Peñaranda, S., Oberste, M.S., Vinjé, J., Koopmans, M., 2011. An automated genotyping tool for enteroviruses and noroviruses. J. Clin. Virol. 51, 121–125. https://doi.org/10.1016/j.jcv.2011.03.006.
Kumar, S., Stecher, G., Li, M., Knyaz, C., Tamura, K., 2018. MEGA X: molecular evolutionary genetics analysis across computing platforms. Mol. Biol. Evol. 35, 1547–1549. https://doi.org/10.1093/molbev/msy096.
Larivé, O., Brandani, J., Dubey, M., Kohn, T., 2021. An integrated cell culture reverse transcriptase quantitative PCR (ICC-RTqPCR) method to simultaneously quantify the infectious concentrations of eight environmentally relevant enterovirus serotypes. J. Virol. Methods 296, 114225. https://doi.org/10.1016/j.jviromet.2021.114225.
Lodder, W.J., Schijven, J.F., Rutjes, S.A., de Roda Husman, A.M., Teunis, P.F.M., 2015. Entero- and parechovirus distributions in surface water and probabilities of exposure to these viruses during water recreation. Water Res. 75, 25–32. https://doi.org/10.1016/j.watres.2015.02.024.
Matsuura, K., Hasegawa, S., Nakayama, T., Morita, O., Uetake, H., 1984. Viral pollution of the rivers in Toyama city. Microbiol. Immunol. 28, 575–588. https://doi.org/10.1111/j.1348-0421.1984.tb00710.x.
Meister, S., Verbyla, M.E., Klinger, M., Kohn, T., 2018. Variability in disinfection resistance between currently circulating enterovirus B serotypes and strains. Environ. Sci. Technol. 52, 3696–3705. https://doi.org/10.1021/acs.est.8b00851.
Morrison, C.M., Hogard, S., Pearce, R., Gerrity, D., von Gunten, U., Wert, E.C., 2022. Ozone disinfection of waterborne pathogens and their surrogates: a critical review. Water Res., 118206 https://doi.org/10.1016/j.watres.2022.118206.
Muckelbauer, J.K., Kremer, M., Minor, I., Diana, G., Dutko, F.J., Groarke, J., Pevear, D. C., Rossmann, M.G., 1995a. The structure of coxsackievirus B3 at 3.5 å resolution. Structure 3, 653–667. https://doi.org/10.1016/S0969-2126(01)00201-5.
Muckelbauer, J.K., Kremer, M., Minor, I., Tong, L., Zlotnick, A., Johnson, J.E., Rossmann, M.G., 1995b. Structure determination of coxsackievirus B3 to 3.5Å resolution. Acta Crystallogr. Sect. D 51, 871–887. https://doi.org/10.1107/S0907444995002253.
Nuanualsuwan, S., Cliver, D.O., 2003. Capsid functions of inactivated human picornaviruses and feline calicivirus. Appl. Environ. Microbiol. https://doi.org/10.1128/AEM.69.1.350-357.2003.
Pattison, D.I., Davies, M.J., 2001. Absolute rate constants for the reaction of hypochlorous acid with protein side chains and peptide bonds. Chem. Res. Toxicol. 14, 1453–1464. https://doi.org/10.1021/tx0155451.
Payment, P., Tremblay, M., Trudel, M., 1985. Relative resistance to chlorine of poliovirus and coxsackievirus isolates from environmental sources and drinking water. Appl. Environ. Microbiol. 49, 981–983.
Pecson, B.M., Darby, E., Danielson, R., Dearborn, Y., Giovanni, G.Di, Jakubowski, W., Leddy, M., Lukasik, G., Mull, B., Nelson, K.L., Olivieri, A., Rock, C., Slifko, T., 2022. Distributions of waterborne pathogens in raw wastewater based on a 14-month, multi-site monitoring campaign. Water Res. 213, 118170 https://doi.org/10.1016/j.watres.2022.118170.

Pennino, F., Nardone, A., Montuori, P., Aurino, S., Torre, I., Battistone, A., Delogu, R., Buttinelli, G., Fiore, S., Amato, C., Triassi, M., 2018. Large-scale survey of human enteroviruses in wastewater treatment plants of a metropolitan area of Southern Italy. Food Environ. Virol. 10, 187–192. https://doi.org/10.1007/s12560-017-9331-3.

Poma, H.R., Kundu, A., Wuertz, S., Rajal, V.B., 2019. Data fitting approach more critical than exposure scenarios and treatment of censored data for quantitative microbial risk assessment. Water Res. 154, 45–53. https://doi.org/10.1016/j.watres.2019.01.041.

Qiao, Z., Wigginton, K.R., 2016. Direct and indirect photochemical reactions in viral RNA measured with RT-qPCR and mass spectrometry. Environ. Sci. Technol. 50, 13371–13379. https://doi.org/10.1021/acs.est.6b04281.

Qiao, Z., Ye, Y., Chang, P.H., Thirunarayanan, D., Wigginton, K.R., 2018. Nucleic acid photolysis by UV254 and the impact of virus encapsidation. Environ. Sci. Technol. 52, 10408–10415. https://doi.org/10.1021/acs.est.8b02308.

Qiao, Z., Ye, Y., Szczuka, A., Harrison, K.R., Dodd, M.C., Wigginton, K.R., 2022. Reactivity of viral nucleic acids with chlorine and the impact of virus encapsidation. Environ. Sci. Technol. 56, 218–227. https://doi.org/10.1021/acs.est.1c04239.

R Core Team, 2019. R: a language and environment for statistical computing.

Rockey, N., Young, S., Kohn, T., Pecson, B., Wobus, C.E., Raskin, L., Wigginton, K.R., 2020. UV disinfection of human norovirus: evaluating infectivity using a genome-wide PCR-based approach. Environ. Sci. Technol. https://doi.org/10.1021/acs.est.9b05747.

Rockey, N.C., Henderson, J.B., Chin, K., Raskin, L., Wigginton, K.R., 2021. Predictive modeling of virus inactivation by UV. Environ. Sci. Technol. https://doi.org/10.1021/acs.est.0c07814.

Rodríguez, R.A., Navar, C., Sangsanont, J., Linden, K.G., 2022. UV inactivation of sewage isolated human adenovirus. Water Res. 218, 118496 https://doi.org/10.1016/j.watres.2022.118496.

Sanjuan, R., Nebot, M.R., Chirico, N., Mansky, L.M., Belshaw, R., 2010. Viral Mutation Rates. J. Virol. https://doi.org/10.1128/JVI.00694-10.

Schijven, J.F., Teunis, P.F.M., Rutjes, S.A., Bouwknegt, M., de Roda Husman, A.M., 2011. QMRAspot: a tool for quantitative microbial risk assessment from surface water to potable water. Water Res. 45, 5564–5576. https://doi.org/10.1016/j.watres.2011.08.024.

Schmidt, P.J., Anderson, W.B., Emelko, M.B., 2020. Describing water treatment process performance: why average log-reduction can be a misleading statistic. Water Res. 176, 115702 https://doi.org/10.1016/j.watres.2020.115702.

Shirasaki, N., Matsushita, T., Matsui, Y., Koriki, S., 2020. Suitability of pepper mild mottle virus as a human enteric virus surrogate for assessing the efficacy of thermal or free-chlorine disinfection processes by using infectivity assays and enhanced viability PCR. Water Res. 186, 116409 https://doi.org/10.1016/j.watres.2020.116409.

Sobsey, M.D., Fuji, T., Shields, P.A., 1988. Inactivation of hepatitis A virus and model viruses in water by free choline and monochloramine. Water Sci. Technol. 20, 385–391.

Sokolova, E., Petterson, S.R., Dienus, O., Nyström, F., Lindgren, P.E., Pettersson, T.J.R., 2015. Microbial risk assessment of drinking water based on hydrodynamic modelling of pathogen concentrations in source water. Sci. Total Environ. 526, 177–186. https://doi.org/10.1016/j.scitotenv.2015.04.040.

Templeton, M.R., Andrews, R.C., Hofmann, R., 2005. Inactivation of particle-associated viral surrogates by ultraviolet light. Water Res. 39, 3487–3500. https://doi.org/10.1016/j.watres.2005.06.010.

Tian, X., Zhang, Y., Gu, S., Fan, Y., Sun, Q., Zhang, B., Yan, S., Xu, W., Ma, X., Wang, W., 2014. New coxsackievirus B4 genotype circulating in inner mongolia autonomous region, China. PLoS One 9, e90379.

Torii, S., Itamochi, M., Katayama, H., 2020. Inactivation kinetics of waterborne virus by ozone determined by a continuous quench flow system. Water Res. 186, 116291 https://doi.org/10.1016/j.watres.2020.116291.

Torii, S., Miura, F., Itamochi, M., Haga, K., Katayama, K., Katayama, H., 2021. Impact of the heterogeneity in free chlorine, UV254, and ozone susceptibilities among coxsackievirus B5 on the prediction of the overall inactivation efficiency. Environ. Sci. Technol. 55, 3156–3164. https://doi.org/10.1021/acs.est.0c07796.

Torrey, J., von Gunten, U., Kohn, T., 2019. Differences in viral disinfection mechanisms as revealed by quantitative transfection of Echovirus 11 genomes. Appl. Environ. Microbiol. AEM 00961. https://doi.org/10.1128/AEM.00961-19, 19.

USEPA, 2002. CT calculator for ground water systems [WWW Document]. URL https://www.epa.gov/dwreginfo/ground-water-rule-compliance-help-water-system-owners-and-operators (accessed 5.30.22).

USEPA, 1989. National primary drinking water regulations: filtration, disinfection; turbidity, giardia lamblia, viruses, legionella and heterotrophic bacteria; final rule.

Verdaguer, N., Jimenez-Clavero, M.A., Fita, I., Ley, V., 2003. Structure of swine vesicular disease virus: mapping of changes occurring during adaptation of human coxsackie B5 virus to infect swine. J. Virol. 77, 9780. https://doi.org/10.1128/JVI.77.18.9780-9789.2003. LP –9789.

Wati, S., Robinson, B.S., Mieog, J., Blackbeard, J., Keegan, A.R., 2018. Chlorine inactivation of coxsackievirus B5 in recycled water destined for non-potable reuse. J. Water Health 17, 124–136. https://doi.org/10.2166/wh.2018.393.

Wigginton, K.R., Kohn, T., 2012. Virus disinfection mechanisms: the role of virus composition, structure, and function. Curr. Opin. Virol. 2, 84–89. https://doi.org/10.1016/j.coviro.2011.11.003.

Wigginton, K.R., Pecson, B.M., Sigstam, T., Bosshard, F., Kohn, T., 2012. Virus inactivation mechanisms: impact of disinfectants on virus function and structural integrity. Environ. Sci. Technol. 46, 12069–12078. https://doi.org/10.1021/es3029473.

Wolf, C., von Gunten, U., Kohn, T., 2018. Kinetics of Inactivation of waterborne enteric viruses by Ozone. Environ. Sci. Technol. 52, 2170–2177. https://doi.org/10.1021/acs.est.7b05111.

Xu, L., Zheng, Q., Zhu, R., Yin, Z., Yu, H., Lin, Y., Wu, Y., He, M., Huang, Y., Jiang, Y., Sun, H., Zha, Z., Yang, H., Huang, Q., Zhang, D., Chen, Z., Ye, X., Han, J., Yang, L., Liu, C., Que, Y., Fang, M., Gu, Y., Zhang, J., Luo, W., Zhou, Z.H., Li, S., Cheng, T., Xia, N., 2021. Cryo-EM structures reveal the molecular basis of receptor-initiated coxsackievirus uncoating. Cell Host Microbe 29, 448–462. https://doi.org/10.1016/j.chom.2021.01.001 e5.

Yasui, M., Iso, H., Torii, S., Matsui, Y., Katayama, H., 2021. Applicability of pepper mild mottle virus and cucumber green mottle mosaic virus as process indicators of enteric virus removal by membrane processes at a potable reuse facility. Water Res. 206, 117735 https://doi.org/10.1016/j.watres.2021.117735.

Ye, Y., Chang, P.H., Hartert, J., Wigginton, K.R., 2018. Reactivity of enveloped virus genome, proteins, and lipids with free chlorine and UV254. Environ. Sci. Technol. 52, 7698–7708. https://doi.org/10.1021/acs.est.8b00824.

Young, S., Torrey, J., Bachmann, V., Kohn, T., 2019. Relationship between inactivation and genome damage of human enteroviruses upon treatment by UV254, free chlorine, and ozone. Food Environ. Virol. https://doi.org/10.1007/s12560-019-09411-2.

Zhong, Q., Carratalà, A., Ossola, R., Bachmann, V., Kohn, T., 2017. Cross-resistance of UV- or chlorine dioxide-resistant echovirus 11 to other disinfectants. Front. Microbiol. 8 https://doi.org/10.3389/fmicb.2017.01928.